SANTIAGO LEÓN VASCO

Sedimentary provenance and low-temperature thermochronology from northwestern Colombia: a record of the Neogene transition from the Panama collision to Nazca subduction controlled tectonics

Short version

Master thesis submitted to the Geosciences Institute of the University of São Paulo to obtain the Master in Science degree.

Area: Geochemistry and Geotectonics

Advisor: PhD. Mauricio Parra Amézquita

São Paulo

2017

Ficha catalográfica preparada pelo Serviço de Biblioteca e Documentação do Instituto de Geociências da Universidade de São Paulo

León Vasco, Santiago
Sedimentary provenance and low-temperature thermochronology from northwestern Colombia: a record of the Neogene transition from the Panama collision to Nazca subduction controlled tectonics / Santiago León Vasco. – São Paulo, 2017.
51 p.: il. + anexos

Dissertação (Mestrado) : IGc/USP
Orient.: Parra Amézquita, Mauricio
Co-orient:

1. Colisão do arco de Panamá 2. Andes do Norte 3. Modelamento termal inverso 4. Proveniência sedimentar 5. Subducção I. Título

Name: Santiago León Vasco

Title: Sedimentary provenance and low-temperature thermochronology from northwestern Colombia: a record of the Neogene transition from the Panama collision to Nazca subduction controlled tectonics

Master thesis submitted to the Geosciences Institute of the University of São Paulo to obtain the Master in Science degree.

Approved on:

Examining Board

PhD. _____

Institution _____

Judgment _____

PhD. _____

Institution _____

Judgment _____

PhD. _____

Institution _____

Judgment _____

Acknowledgements

This research was financially supported by the Fundación para la Promoción de la Investigación y la Tecnología (FPIT) – Banco de la República de Colombia (Project 3809), and by the ACGGP-Ares Corrigan Fund (Project Paleogene Accretion-Deformation in Western Colombia: Implications in South-American Continental Growth and Andean Orogeny).

Professor Agustín Cardona Molina from the Universidad Nacional de Colombia, and Juan Sebastián Jaramillo, are specially acknowledged. Their strong academic support and their sincere friendship undoubtedly improved each detailed involved in the materialization of this manuscript. Every single member of the EGEO research group is also acknowledged.

I thank Professor Mauricio Parra for accepting me as his former graduate student at the University of São Paulo, and for the access to his recently constituted Laboratório de Termocronologia de Baixa Temperatura (LABTER).

CAPES provided the scholarship that allowed me to complete this research project.

I am grateful to Ed Sobel from the University of Potsdam, for providing the Apatite (U-Th)/He analyses. I am also thankful to Victor Valencia from the Washington State University for providing the U-Pb geochronological analyses. Professor Andrés Pardo Trujillo is acknowledge for sharing U-Pb detrital geochronology data used in this work.

Suggestions and discussion with Sebastián Echeverri certainly benefited this research.

I would like to thank Ana María Patiño, and the staff from the Instituto de Energia e Ambiente, and the Instituto de Geociências for their help during sample preparation.

Finally, I thank Professor Claudio Ricommini for his help during my application to the master program.

Abstract

The occurrence of major plate reorganization during the Neogene, reflects the complex interactions between the Caribbean, Farallon and South-American plates, and the Panama Arc. These, have influenceed the tectono-stratigraphic record of the northwestern Colombian Andes, which has been scarcely studied neart the suture between the Panama and South-American domains. New sandstone petrography, heavy minerals analyses, U-Pb detrital zircon geochronology, whole-rock geochemical data, and thermal inverse modeling of multiple thermochronometers, carried along a 50 km southeast-northwest transect, allow to reconstruct the deformation and exhumation/erosional history of the Late Cretaceous to Pliocene rocks from the western flank of the Western Cordillera. The onset of exhumation of Late Cretaceous sedimentary rocks, associated with the South-American margin, occurred between 45-20 Ma, as suggested by the initial cooling from temperatures within the zircon helium partial retention zone (ZPRZ, ~180-200°C). These rocks also experienced a substantial pulse of exhumation during the Middle Miocene, which is characterized by moderately rapid rates between ~0.3 km/my and 0.7 km/my. Moreover, a Pliocene period of rapid cooling is also documented with maximum exhumation rates of ~1.3 km/my. The Middle Eocene rocks from the intra-oceanic Panama Arc, which are separated by a highly-deformed zone from the Late Cretaceous rocks of the Western Cordillera, record an initial cooling at ca. 15 Ma from the apatite partial retention zone (APRZ, ~80-60°C) at rates around 0.6 km/my. Detrital thermochronology of post-collisional sequences and modern river sediments also record these exhumation events. The we results can be related to more regional-scale tectonic processes including: the Late Oligocene rapid and frontal convergence between the newly formed Nazca plate and the continental South-American plate following the fragmentation of the former Farallon plate, the Middle Miocene collision of the Cretaceous-Eocene Panama Arc that triggered generalized exhumation-deformation widespread in the upper NW South-American plate, and the Middle to Late Miocene initiation of the Nazca subduction and installation of a Late Miocene-Pliocene flat-slab to the north. The latter is likely to represent the mechanism that triggered surface uplift in eastern Colombia and ongoing uplift-deformation of western coastal ranges and eastern foreland basins north of 5°N

Keywords: Panama arc collision, Northern Andes, Inverse thermal modeling, sedimentary provenance, subduction.

Resumo

A ocorrência de uma grande reorganização de placas durante o Neógeno reflete a comlpexa interação entre as placas do Caribe, Farallon, e América do Sul, e o arco intra-oceânico de Panamá. Isto, tem influenciado o registro tectono-estratigráfico dos Andes nor-ocidentais da Colômbia, o qual tem sido escassamente estudado perto da sutura entre os domínios de Panamá o da América do Sul. Novos dados de petrografia de arenitos, análises de minerais densos, geocronologia detrítica em zircão, geoquímica de rocha total, e modelamento termal inverso de múltiplos termocronômetros, realizados em um transepto de 50 km com direção SE-NW, permitem reconstruir a história de deformação e exumação/erosão das rochas do Cretáceo Superior ao Plioceno do flanco ocidental da Cordilheira Ocidental. O início da exumação das rochas do Cretáceo Superior associadas com a margem continental Sul-americana, ocorreu entre 45 e 20 Ma, o qual é sugerido pelo resfriamento inicial desde temperaturas dentro da zona de retenção parcial do hélio em zircão (~180-200°C). Essas rochas, também sofreram um pulso de exumação considerável durante o Mioceno Médio, o qual caracteriza-se por taxas moderadamente rápidas entre 0.3 km/my e 0.7 km/my. Adicionalmente, um período de resfriamento rápido também é documentado com taxas máximas de exumação ~1.3 km/my. As rochas do Eoceno Médio do arco oceânico de Panamá, as quais estão separadas das rochas do Cretáceo Superior da Cordilheira Ocidental por uma faixa de deformação, registram um resfriamento inicial em ~15 Ma desde a zona de retenção parcial de hélio em apatita (APRZ, ~80-60°C, com taxas perto de 0.6 km/my. Termocronologia detrítica em secuências pós-colisionais e sedimentos modernos, também registram estes períodos de exumação. Os novos resultados podem ser relacionados com processos tectônicos de escala regional, que incluem: Convergência rápida e frontal no Oligoceno Superior, entre a recentemente formada placa de Nazca e a placa continental Sul-americana, depois da fragmentação da antiga placa de Farallon, a colisão do Arco de Panamá do Cretáceo Superior-Eoceneo durante o Mioceno Médio, o qual resultou exumação geral ao longo do segmento NW da placa Sul-americana, é o início da subducção da placa de Nazca é a instalação de um segmento plano ao norte durante o Mioceno Superior-Plioceno. Este é provavelmente o mecanismo responsável pelo soerguimento da superfície recente na Colômbia nor-oriental e a contínua deformação-soerguimento das serras costeiras ocidentais e das bacias orientais de foreland ao norte de 5°N.

Palavras chave: Colisão do arco de Panamá, Andes do norte, Modelamento termal inverso, Proveniência sedimentar, Subducção

Table of Contents

List of figures

1. Introduction

The northern Andes have been considered as a particular segment of the entire South-American chain, since its Meso-Cenozoic growth has been influenced by the accretion of oceanic terranes, such as island-arcs, oceanic plateaus, seamounts or offscraped sediments from the subducting plate, interspersed with different phases of oceanic crust subduction (Gansser, 1973; Ramos, 1999).

These changing tectonic settings result from the complex interaction between the Caribbean, Farallon and South-American plates (Bayona et al., 2012; Cardona et al., 2011; Pindell and Kennan, 2009; Spikings et al., 2015) that is also responsible for the middle Miocene collision of the Panama Arc and the subsequent Isthmus closure that constitutes one of the most influencing phenomena on the modern oceanographic and biogeographic global configuration (Coates et al., 2004; Duque-Caro, 1990a, 1990b; Escalona and Mann, 2011; Ibaraki, 1997; Iturralde-Vinent and MacPhee, 1999; Montes et al., 2015; Tsuchi, 1997; Webb, 2006)

The growing of accretionary orogens like the northern Andes is characterized by the incorporation of oceanic crust of different age composition and thickness, generation of magmatic arcs and the formation of distinct types of upper-plate sedimentary basins (i.e. back-arc, forearc, marginal and foreland basins) (Cawood et al., 2009; Kusky et al., 2013; Pubellier and Meresse, 2013). The continuous accretion of these elements and changes in characteristics and factors controlling the geometry of the subduction zone (i.e. slab-dip, obliquity, convergence rates, and structural inheritance) is responsible for the over-imposition of multiple magmatic, sedimentary and deformation events, which requires appropriate temporal constraints and an integrated multi-technical approach in order to be reconstruct the overlapped tectonic facies (Boutelier et al., 2012; Cloos, 1993; Spikings and Simpson, 2014; von Huene and Scholl, 1991).

Although major advances have been made in order to recognize the timing of the establishment of an emerged Central American land-bridge beteen South and North America, and its implications on ecological and environmental phenomena, the timing and nature of the

geological processes involved are still matter of debate (i.e. collision of the Panama Arc, subduction of the Nazca and Cocos plate) (Farris et al., 2011; Lonsdale, 2005; Mann, 1995; Vannucchi et al., 2006; Wegner et al., 2011; Whattam et al., 2012). Therefore, ages ranging from 23 Ma and ca. 3 Ma, have been proposed for both the early interaction ant the ultimate establishment of a land connection between the Americas. (Bacon et al., 2015; Coates et al., 2004; Duque-Caro, 1990a, 1990b; Montes et al., 2015; O' Dea et al., 2016).

In this contribution, we present integrated field observations, sedimentary provenance, U-Pb geochronology, geochemistry of magmatic rocks and low-temperature thermochronology analyses, carried out throughout a ~50 km-long NW-SE transect between the axis and western flank of the Western Cordillera of Colombia. This transect crossed the Uramita Fault Zone, which represent a major expression of the suture between the Panama Arc and South-American margin (Duque-Caro, 1990a; Toussaint and Restrepo, 1994) (**Figure 1**).

The integration of this multidisciplinary approach, together with published geochemical, geochronological, stratigraphic, and thermochronological constraints from western Colombia are used to reconstruct different tectonic scenarios that shaped the continental margin during the Neogene. We specifically attempt to differentiate the Panama and South-American blocks by means of contrasting their provenance and particular geochemical signature and to identify periods of rapid exhumation and deformation potentially conditioned by their structuration, and correlate them with global and local plate kinematic models for the Neogene.

The new results presented here elucidate a more complicated Mio-Pliocene tectonic scenario of transition from collisional to subduction-dominated regimes, which must be considered when the paleogeographic and tectonic models of the interaction between South-America and the Panama Isthmus are discussed.

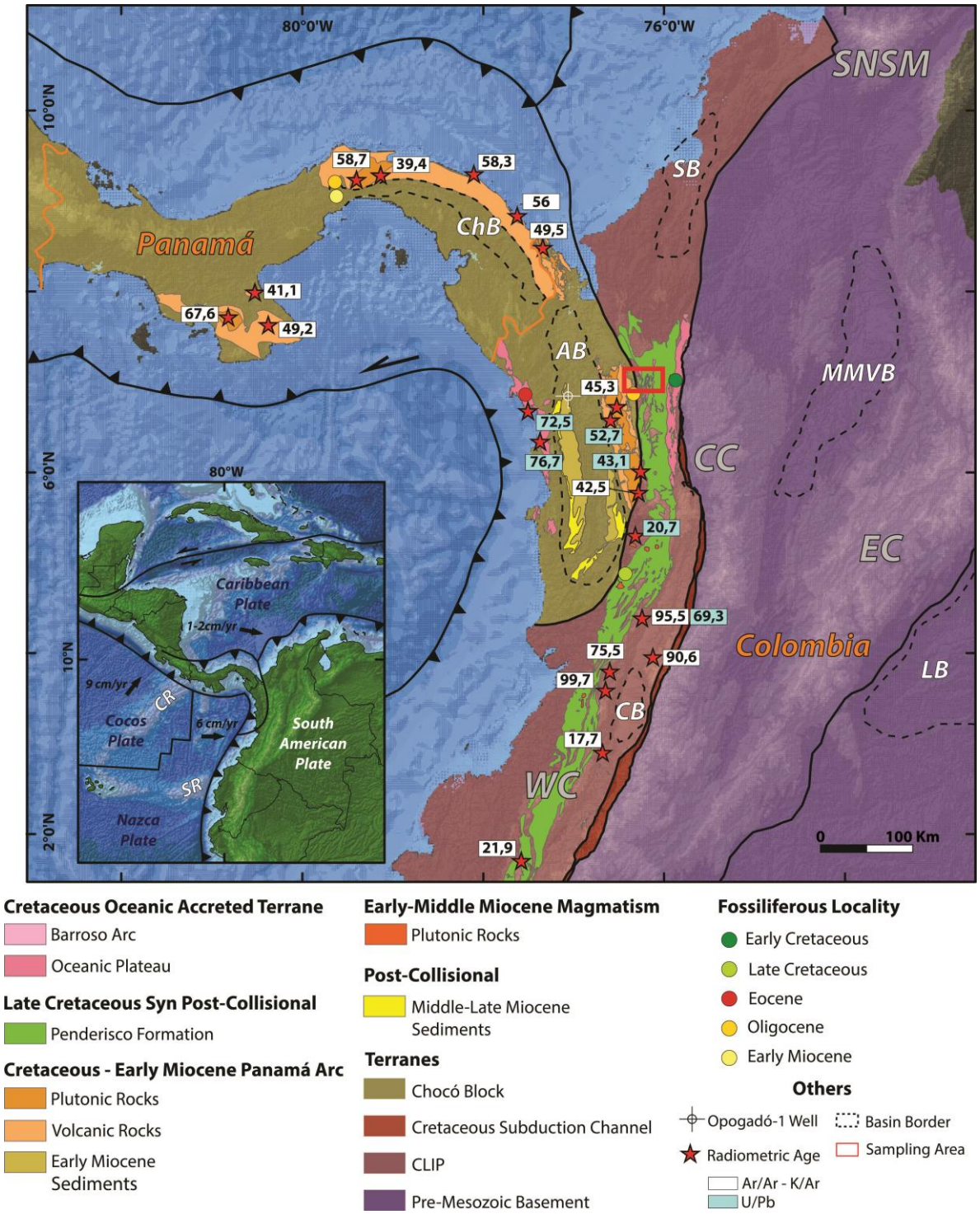

Figure 1. Regional tectonic map and main geological features considered for discussion. Geological data compiled from (Gómez et al., 2015; Montes et al., 2012a, 2012b; Rodríguez et al., 2013; Valencia-Giraldo et al., 2016).

2. Geological framework

The over-imposition of b-type subduction of oceanic crust and the accretion of exotic terranes, has imprinted a peculiarity to the evolution of the Colombian and Ecuadorian Andes (Gansser, 1973; Ramos, 1999; Restrepo and Toussaint, 1988) with respect to the central and southern segments, where mountain building and continental growth are solely controlled by subduction processes (Kay and Coira, 2009; Ramos, 2010). Since the Eocene, the NW corner of South-America has been affected by major plate re-adjustments, including changes in plate convergence obliquity (Bayona et al., 2012), breaking-up of the former Farallon oceanic plate and formation of the Nazca and Cocos plates (Lonsdale, 2005), the arc-continent collision with the Panama Arc (Duque-Caro, 1990a; Montes et al., 2015), and the apparent onset of a flat-slab subduction in northern Colombia (Chiarabba et al., 2015; Syracuse et al., 2016). Such major changes are recorded in the filling and deformation of the Late Cretaceous-Pliocene sedimentary basins exposed along the northwestern flank of the Western Cordillera of Colombia and the Atrato Valley (**Figure 1**). However, in contrast with the great amount of thermochronological, structural, sedimentological and stratigraphic analysis carried out in the Eastern and also in the Central Cordillera of Colombia (Parra et al., 2012, 2010, 2009b; Reyes-Harker et al., 2015; Spikings et al., 2015; Villagómez et al., 2011; Villagómez and Spikings, 2013), limited rock exposure obscured by a dense vegetation cover, deep soil profiles, and limited access roads, including political conflicts, have complicated the acquisition of similar data in western Colombia. Such situation hinders the proposition of integrative models that allows understanding the upper-plate effects from the forearc to the foreland regions, associated with the different tectonic scenarios experienced by the continental margin during the Neogene.

In this section, we summarize the major regional tectonic events that may have affected the continental margin of northern South-America since the Oligocene and discuss the relation that such events apparently have with the geological record.

We present a summarized tectono-stratigraphic chart that allows comparing the timing and nature of major changes in sedimentary facies within the forearc, intermontane, and foreland

basins of Colombia. We also highlight the periods of ongoing exhumation in the adjacent mountain ranges (**Figure 2**).

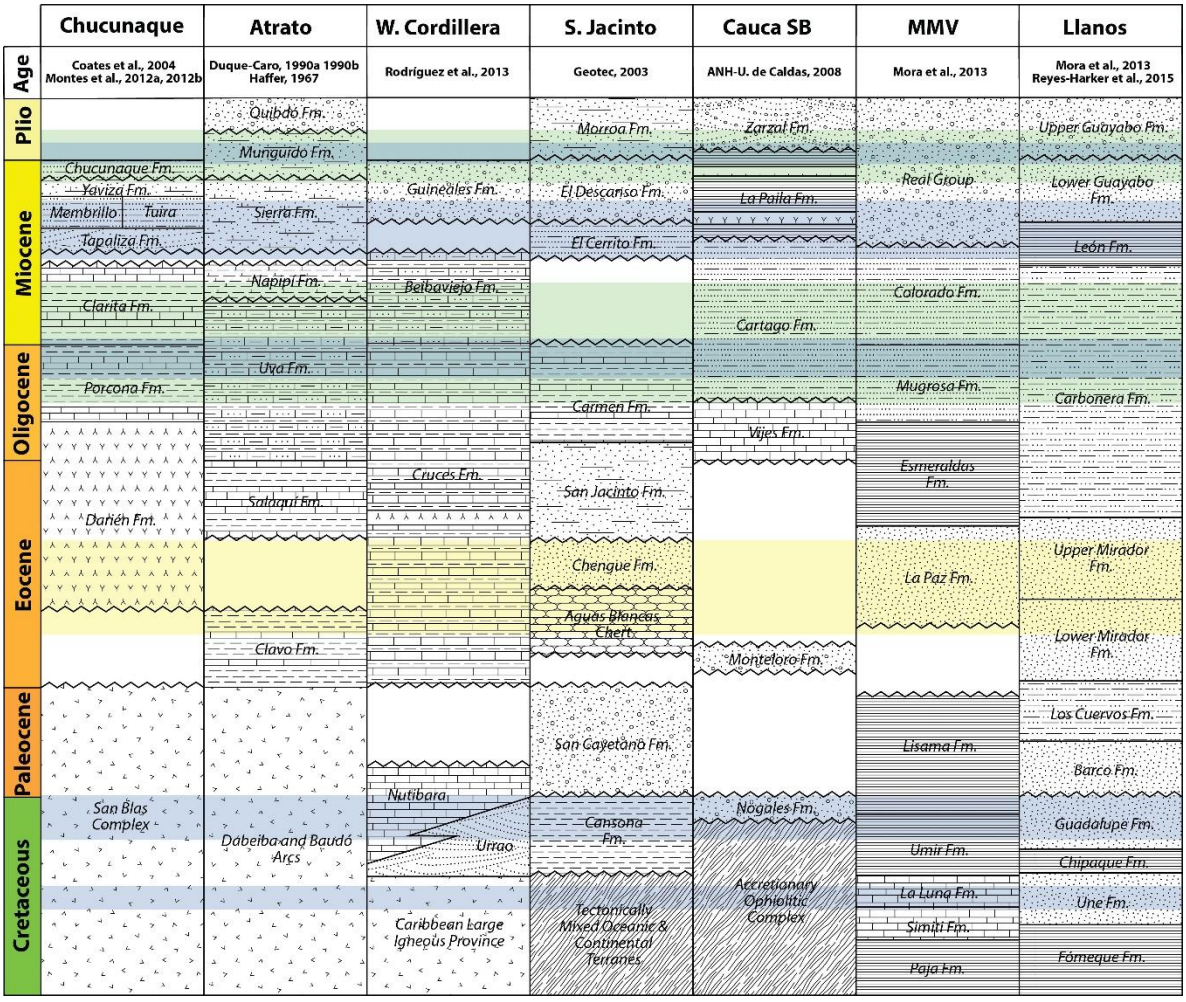

Figure 2. Summarized tectono-stratigraphic chart for the main sedimentary basins of Colombia. Shaded zones indicate periods of moderate to rapid exhumation: blue (Central Cordillera), yellow (Panama Arc), Green (Eastern Cordillera). Data is compiled from (ANH-Universidad de Caldas, 2008; Coates et al., 2004; Duque-Caro, 1990a, 1990b; Geotec, 2003; Haffer, 1967; Montes et al., 2012a, 2012b; Mora et al., 2013; Reyes-Harker et al., 2015; Rodríguez et al., 2013; Villagómez and Spikings, 2013).

2.1. Farallon break-up

The fragmentation of the Farallon plate and the consequent formation of the Cocos and Nazca plates took place at ca. 23 Ma (Lonsdale, 2005). Such event was responsible for changes in the convergence angles (increased orthogonality) and rates between the newly formed Nazca

oceanic plate and the South-American margin, which apparently reached the highest Cenozoic values around 15 cm/yr (Pardo-Casas and Molnar, 1987; Somoza, 1998; Somoza and Ghidella, 2012). Some authors have suggested that this event might be a controlling mechanism for moderately-rapid exhumation observed in a thermochronological age-elevation profile carried out in the Cretaceous plutons of the northern Central Cordillera (Restrepo-Moreno et al., 2009). Whereas based on stratigraphic, thermochronometric and structural analyses, a period of rapid exhumation has been identified on the Eastern Cordillera during that time (Horton et al., 2010; Mora et al., 2013; Parra et al., 2009a; Reyes-Harker et al., 2015). Arc magmatism seems to become important during the Late Oligocene-Early Miocene (Schütte et al., 2010) and followed a Late Eocene magmatic hiatus in the Colombian Andes (Bayona et al., 2012)

2.2. Middle to Late Miocene docking of the Panama Arc

The Miocene evolution and continental growth of the NW corner of South-America have been mainly related to the collision of the Panama Arc against the NW Andean continental margin, and the subsequent re-establishment of a subduction zone (Duque-Caro, 1990a). This oceanic terrane is composed of Late Cretaceous-Eocene magmatic rocks geochemically akin with an island arc setting, which were constructed over an Early to Late Cretaceous oceanic plateau probably linked with the *Caribbean Large Igneous Province* (CLIP) (Burke, 1988; Kerr et al., 1996; Sinton et al., 1998). Volcanic and plutonic rocks from the Santa Cecilia-La Equis Complex, and the Mandé and Acandí batholiths in the Western Cordillera, and other correlatable units in Panama, constitute this domain (Buchs et al., 2011, 2010; Kerr et al., 1997; Montes et al., 2012a; Wegner et al., 2011; Wörner et al., 2009) (**Figure 1**). The tectonic limit that marks the suture zone of this block in NW Colombia, referred as the Uramita Fault Zone (Duque-Caro, 1990a) or the Dabeiba-Pueblo Rico Fault (Toussaint and Restrepo, 1994), is defined by a regional fault-system with quaternary activity, whose southern tip is characterized by the occurrence of a high-strain zone (Istmina deformed belt) (Cediel and Shaw, 2003; Duque-Caro, 1990a; Noriega-Londoño et al., 2013)

As suggested above, no consensus has been achieved in the scientific community on the timing and nature of the geological processes involved in the collision of the Panama Arc with the NW

Andes. In fact, we claim that one of the main issues could be anchored to the confusion related to terms used to refer some specific phenomenon (seaway closure, full establishment of a land-bridge, tectonic collision that drives rock cooling and exhumation). Within this scenario, ages that span from 23 Ma to 3 Ma, which individually are interpreted to document one of those phenomena above-mentioned, are cited together when discussing in a general way the timing of the formation of the Panama isthmus and its collision and connection with northwestern South-America (Bacon et al., 2015; Duque-Caro, 1990a; Montes et al., 2015; O' Dea et al., 2016; Pindell and Kennan, 2009).

The Eocene to Pliocene strata deposited in the Atrato Basin in NW Colombia and the Chucunaque-Tuira Basin from SE Panama, include a series of unconformities, shallowing of sedimentary environments, and switching from marine to nonmarine sedimentation, which initiate in the Middle Miocene (Coates et al., 2004; Duque-Caro, 1990a, 1990b; Haffer, 1967; Montes et al., 2012b; Ramírez et al., 2016), and are probably influenced by the ongoing collisional event at ca. 15 Ma. that also potentially influenced the occurrence of subsequent orogenic uplift and deformation inboard the continent as suggested for the accumulation of thick syn-tectonic conglomeratic sequences, increased sedimentation rates, and regional unconformities identified in foreland and intermontane basins in eastern Colombia (Gómez et al., 2005, 2003; Mora et al., 2013; Pardo-Trujillo et al., 2015; Reyes-Harker et al., 2015; Rodríguez et al., 2016; Suter et al., 2008).

2.3. Mio-Pliocene subduction-dominated tectonics

Widespread upper-plate magmatism since the Middle-Late Miocene (ca. 13 Ma) in northwestern South-America, indicates the establishment of a renewed continental arc following the re-initiation of subduction of the Nazca oceanic plate underneath South-America after the accretion of the Panama Arc (Leal-Mejía, 2011; Rodríguez-García and Bermúdez-Cordero, 2015; Rodríguez and Zapata, 2012; Zapata and Rodríguez, 2011).

Based on the seismicity registered by the Colombian national network, Chiarabba et al. (2015) and Syracuse et al. (2016) have proposed the existence of a flat-slab subduction beneath the

Eastern Cordillera northward of 5°N. The Late Miocene-Pleistocene ongoing deformation in the foreland basins (Veloza et al., 2015), regional uplift of the Eastern Cordillera (Mora et al., 2013; Parra et al., 2009a), together with shallowing of forearc basins (Duque-Caro, 1990a, 1990b; Haffer, 1967), and exhumation of the northern segment of the Western Cordillera (Pardo-Trujillo et al., 2015; Restrepo-Moreno et al., 2015), took place during this time interval and therefore, may suggest a causal link with the flat-slab configuration, that needs to be evaluated.

The new results from the selected transect in western Colombia, will allow testing if these distinct tectonic scenarios are constrained in the hinterland, near the suture of the Panama Arc

3. Methods

3.1. Fieldwork

The study area is comprised between the localities of Cañasgordas and Dabeiba, approximately 170 kilometers west of the city of Medellín (**¡Error! No se encuentra el origen de la referencia.**).The main lithological and structural features of the rock units cropping out along an SE-NW oriented cross-section of ca. 50 km long and 5 km wide were described in ~100 field stations. Ninety-seven samples were collected during this stage, and representative samples from each major geological unit were selected for further analyses. Locations, lithological units and analytical methods applied for all samples are summarized in **Appendix 1**.

3.2. Petrography

Forty thin sections, including magmatic and sedimentary rocks from all mapped units, were analyzed. Characteristic compositional and textural features of each sample were described using an Olympus BX51 polarizing microscope at the Laboratory of Low-Temperature Thermochronology (LABTER) of the Instituto de Energia e Ambiente of the Universidade de São Paulo. Modal mineral proportions of igneous rocks were determined by point-counting of at least one hundred grains on each sample. Petrographic analyses of magmatic rocks were also used to determine the grade of alteration, which was considered when interpreting the whole-rock geochemistry data. Petrographic analyses of seventeen sedimentary rocks from the Penderisco, Cruces and Beibaviejo formations, where done by counting of at least 400 points including framework, matrix and cement, and following methods suggested by Dickinson (1985), Folk (1980), and Garzanti (2016).

3.3. Conglomerate clast-counting

During the field work, four localities of the Late Miocene Guineales Formation were clast-counted using the ribbon method (Howard, 1993). A total of one-hundred clasts with a diameter greater than 2 cm were counted to assess the sedimentary provenance of this unit.

3.4. Heavy Minerals Analyses

Eleven sandstone samples were crushed, sieved and hydraulically concentrated on the Wilfley table. The 63-250 μm fraction was selected to minimize the hydraulic sorting effect and the apparent discrepancies between mineral proportions induced by the presence of large grain-size differences on the mounts (Mange and Maurer, 1992; Morton, 1985). Subsequently, minerals with a density above 2.89 gr/cm^3 were obtained using sodium polytungstate. Mounts were prepared using the Meltmount ® resin with a refraction index of 1.539. At least 300 translucent grains were optically identified following the ribbon method (Mange and Maurer, 1992). Additionally, apatite and zircon concentrate for U-Pb geochronology, and fission-track and (U-Th)/He thermochronology analysis, were obtained by magnetic separation and using di-iodomethane (3.32 gr/cm^3).

3.5. U-Pb Geochronology

LA-ICP-MS U-Pb analyses were obtained from three samples at the Washington State University Geoanalytical lab, using a New Wave Nd: YAG UV 213-nm laser coupled to a ThermoFinningan Element 2 single collector, double-focusing, inductively coupled plasma-mass spectrometer (ICP-MS), according to procedures described in (Chang et al., 2006). The Plešovice zircon with an age of 337.13 ± 0.37 Ma (Sláma et al., 2008), was used as a standard during the analysis. Laser spot-size and repetition rates were 30 μm and 10 Hz respectively. Each analysis consisted of a short blank analysis followed by 250 sweeps of 30 s through masses 202, 204, 206, 207, 208, 232, 235 and 238. Fractionation was corrected by normalizing U/Pb and Pb/Pb ratios of the unknowns to the zircon standards (Chang et al., 2006). U and Th abundances were monitored by comparison to NIST 610 trace-element glass. U-Pb ages were calculated using Isoplot 4.15 (Ludwig, 2003). We also used the Excel macro available from the Arizona Laserchron Center (www. geo.arizona.edu/alc), in order to identify the age peaks present in the detrital samples. Individual ages older than 150 Ma that exceeded 20% of discordance were discarded. No filter was applied for ages younger than 150 Ma, given the difficult of determining robust $^{207}Pb/^{206}Pb$ ages (Gehrels, 2012).

3.6. Whole-rock geochemistry

Whole-rock geochemical analyses of five magmatic rocks from the Santa Cecilia-La Equis Complex were conducted at the ALS Minerals laboratories in Lima, Peru.

After crushing, splitting and pulverizing, an aliquot of 0.1 g is added to a $LiBO_2$ / $Li_2B_4O_7$ flux, mixed and fused in a furnace at 1000°C. The resulting melt is then cooled and dissolved in 100 mL of 4% HNO_3 / 2% HCl. This solution is then analyzed for major oxides by inductively coupled plasma – atomic emission spectroscopy (ICP-AES) and the results are corrected for spectral inter-element interferences. For trace and rare-earth elements, an aliquot of 0.1 g is added to a $LiBO_2$ / $Li_2B_4O_7$ flux (1.8 g), mixed and fused in a furnace at 1025°C. The resulting melt is cooled and dissolved in a mixture containing HNO_3, HCl, and HF. This solution is then analyzed by ICP-MS. Data handling, plotting, and interpretation were performed using the software GCD Toolkit 4.1. (Janoušek et al., 2006). Additionally, a compiled database of ~270 geochemical analyses from rocks exposed along the Western Cordillera of Colombia and Panama, were used to compare the new data presented here, and look for an appropriate discrimination of the main magmatic units (Buchs et al., 2010; Farris et al., 2011; Kerr et al., 1997; Montes et al., 2012a; Rodríguez et al., 2012; Rodríguez and Arango, 2013; Villagómez et al., 2011).

3.7. Low-temperature thermochronology

Aiming to reconstruct the thermal history of the Late Cretaceous to Miocene rocks exposed on the northwestern segment of the Western Cordillera, we implemented a multi-thermochronometer approach on each representative unit present in the study area (**¡Error! No se encuentra el origen de la referencia.**). Combined apatite fission-track (AFT) with apatite and zircon (U-Th)/He analyses were employed to unravel the T-t evolution of the northwestern Andes between the ~180° and 60° isotherms gave the suggested closure temperatures for these systems (Reiners and Brandon, 2006). Hence, the exhumation history through upper-crustal depths could be assessed.

3.7.1. Zircon (U-Th)/He dating (ZHe)

Daughter He and parent U-Th nuclides were measured at the University of Arizona following the procedures of Reiners (2005). Preferably tetragonal, inclusion-free zircon grains with prism widths >75μm were hand-picked and packed into a slightly closed ~1 mm Nb foil. Before packing, two dimensions perpendicular to the a_1 and a_2 crystallographic axes of the selected grains were measured, and its morphology described in order to calculate the alpha-ejection correction (Farley, 2002; Farley et al., 1996) Subsequently, foil packets were placed on a Cu planchet in a high-vacuum chamber connected to the He purification-measurement line. Each Nb foil was heated to ~1100°C-1250°C by focusing a 10 μm Nd-YAG 1064 nm laser beam, for 15 min extraction intervals. At least two re-extractions were performed for each sample to assess the extent of degassing of the crystal. The $^{4}He/^{3}He$ ratio is measured following gas release and nominal equilibration time. Measured ratios were corrected for background and interferences on mass 3 (HD+ and H3+) and then compared with $^{4}He/^{3}He$ measured on pipetted aliquots of a manometrically calibrated ^{4}He standard. U and Th parent nuclides in degassed zircons were measured by isotope dilution and solution ICP-MS. This method requires spiking with an isotopically distinctive U-Th spike, sample spike equilibration, and dissolution to a final solution appropriate for ICP-MS. Zircon dissolution was attained using HF-HNO_3 mixtures in Parr bombs, which can entirely dissolve the Nb foils. $^{238}U/^{233}U$ and $^{232}Th/^{229}Th$ ratios were quantified by 2000 measurements of the average intensities in the middle 10% of peak-widths in low-resolution mode on an Element2 high-resolution ICP-MS. Pt contamination and mass fractionation were checked measuring the $^{238}U/^{235}U$ ratio. U and Th abundances were calculated from multiple determinations of isotope ratios on a pure spike and spiked normal containing 1-4 ng of isotopically normal U and Th. A 2σ uncertainty is reported for all ages. The potential effect of radiation damage on the ZHe data dispersion was assessed by comparing the effective uranium e[U] with individual ages, following the model of (Flowers et al., 2007) and (Guenthner et al., 2013)

3.7.2. Apatite fission-track (AFT) analyses

AFT analyses were conducted on 6 samples collected along the studied section following the External Detector Method (EDM) (Gleadow, 1981). A detailed description of this method, as well as its theoretical principles, is presented in **Appendix 1**.

Apatite concentrates were mounted in an epoxy resin and polished to expose the internal grains surfaces. Mounts were chemically etched in 5.5 HNO_3 for 20 s at 20°C ± 1°C to reveal spontaneous fission-tracks. After the attaching of the external detector low-U mica, samples were irradiated at the Oregon State University research reactor. Subsequently, induced fission-tracks were revealed by etching with 40% hydrofluoric acid at 21°C for 45 min. Spontaneous and induced fission-tracks density were determined at the Low-Temperature Thermochronology Lab of the University of São Paulo using an Olympus BX51 microscope with a digitalizing tablet and a coupled computer-controlled stage driven by the FTStage 4.05 software (Dumitru, 1993). Ages and errors were calculated using the zeta calibration method (Hurford and Green, 1983) with the Trackkey software (Dunkl, 2002). A zeta calibration factor of 126.5 ± 4.1 (CN1 glass; Santiago León) was used. Chi-square test was used to evaluate whether individual ages belong to a unique population. Datasets with a $P(\chi^2) > 5\%$ are considered to represent a concordant age (Galbraith, 1981). The software DensityPlotter version 7.3 were used as a visualization tool for detrital and non-detrital samples (Vermeesch, 2012, 2009). The Kernel Density Estimator (KDE) was used to evaluate the detrital AFT age distribution, a bandwidth of 5 Ma was chosen in order to avoid over- or under-smoothing (Vermeesch, 2012).

3.7.3. Apatite U-Th/He (AHe) dating

Five samples were selected for AHe. Four to five individual apatite grains for each sample were hand-picked, photographed and packed in 1 mm Pt tubes using an Olympus SZX16 stereo microscope following the procedure suggested by Farley (2002). Grain dimensions and the number of terminations were determined to calculate the retentivity (F_T) correction factor (Farley et al., 1996). The platinum tubes were loaded into a 25-spot laser chamber of an ASI Alphachron He extraction and analysis system, equipped with a 30W Coherent 978 nm diode

laser and a Pfeiffer Prisma 200 Quadrupole mass spectrometer, at the University of Potsdam, Germany. Routinely, blank tubes and age standards were analyzed together with unknown samples. Samples were heated by the laser system at 8 amps (~3.5W) for 5 minutes to release all He from the apatite grains. After exposing for 1 minute to a hot getter, designed to remove chemically active gas species, the released gas after heating was purified. The abundance of ^{4}He in the purified gas was measured by isotope dilution using a ^{3}He tracer, calibrated against a manometrically determined ^{4}He standard. A second analysis or re-extraction was done for each sample in order to ensure that the grain was completely degassed. Analysis of U, Th and Sm were carried at the clean lab at GFZ Potsdam by isotope dilution ICP-MS. Samples were placed in 3ml Savillex PFA screw-cap vials, spiked with an HNO_3-based ^{235}U-^{230}Th spike and an HNO_3-based ^{149}Sm spike, and dissolved with a ~0.5 ml 7N HNO_3. The spikes were calibrated against NIST-traceable Certified Reference Material ICP concentration standards. Aiming to ensure the total sample dissolution and isotopic homogenization between sample and spikes, the vials were placed on a hotplate at ~100°C for at least 24 hours. The solution was then evaporated to dryness and re-dissolved for another 24 h in 1.5 ml 2% HNO_3. Then, the solution was analyzed for U, Th, and Sm isotopic composition on a Thermo Element 2 XR ICP-MS at GFZ Potsdam, equipped with a CETAC ASX-520 auto-sampler system, and run in the low-resolution mode to maximize transmission of ions. Mass 234 was also analyzed to detect potential Pt-Ar isobaric interferences on the U mass spectrum. Repeated analyses of $^{149}Sm/^{147}Sm$ ratio, and of the NIST SRM material U-500, were used to monitor instrumental mass fractionation. Age calculations followed the procedure of (Meesters and Dunai, 2005). A 2σ uncertainty is reported for all ages.

The potential effect of radiation damage on AHe data was assessed by comparing the effective uranium e[U] with individual ages, following the model of (Flowers et al., 2007).

3.7.4. Thermal Modeling

Thermal modeling was performed using the HeFTy v. 1.80 software. Input data include AHe, ZHe, fission-track ages, track lengths when available, and Dpar as a kinetic parameter. Between 20000 and 195000 iterations were done using a Monte-Carlo search method, until at least 20 to

50 good models (Goodness of Fitness > 0.5) were obtained (Ketcham, 2005). For fission-track annealing, we used the kinetic model of (Ketcham et al., 2007), for AHe and ZHe we used the models of (Farley, 2000) and (Guenthner et al., 2013) respectively.

Additional constraints, as stratigraphic ages and provenance criteria, were included allowing the software to search for a wide range of a coherent T-t spectrum. For discussion an estimation of burial/exhumation rates, we use a geothermal gradient of 15°C/Km, which has been suggested as a mean value for subduction-related settings (Dumitru, 1991; Henry and Pollack, 1988).

4. Conclusions

The integration of new sedimentary provenance, whole-rock geochemical analyses, and thermochronological data, together with regional tectono-stratigraphic and geochronological constraints along an east to west transect in the northwestern segment of the Western Cordillera allows to reconstruct the exhumation/deformation periods that affected the South-American continental margin since the Oligocene, and explore the potential causal link between these events with the over-imposition of collisional and subduction dominated tectonics. The new results suggest that the construction of the Late Cretaceous continental margin was initially controlled by the accretion of an Early to Late Cretaceous oceanic plateau, on which syn to pos-collisional sediments from the Penderisco Fm. were accumulated. Protracted burial of this sedimentary sequence was followed by a period of contractional tectonics that triggered the onset of its exhumation/cooling from depths equivalent to temperatures within the zircon helium partial retention zone (ZPAZ, ~180-200°C) at any time between 45-20 Ma, which overlaps with a period of high tectonic instability in eastern Colombia, and with the suggested age for the Farallon plate break-up and the subsequent formation of the Cocos and Nazca plates. A subsequent pulse of moderately-rapid exhumation (~0.3 to 0.7 km/my) at ca. 15 Ma of the Early to Late Cretaceous of the Western Cordillera, is also constrained by the new AFT ages. This Middle Miocene pulse of exhumation is also registered by cooling of the volcano-clastic rocks from the Eocene Cruces Fm. from temperatures within the apatite helium partial retention zone (APAZ, ~60-80°C), as suggested by the AHe ages ca. 14 Ma obtained from this unit. A period of combined increased sedimentation rates and uplifting of the forearc Atrato Basin at ca. 15 Ma, correlates well with the pulse of exhumation/erosion documented for the adjacent orogens. The above together with changes in the sedimentary and provenance patterns on intermontane and foreland basins of eastern Colombia indicates a period of intense tectonic activity during the Middle-Late Miocene in the northern Colombian Andes. The collisional nature of this event is suggested by the mixed U-Pb detrital ages of sediments being accumulated at this time, that include both pre-Mesozoic continental-basement signature and Late Eocene ages, which are uniquely sourced from the intra-oceanic Panama Arc. The suture zone between this accreted oceanic terrane and the South-American continental margin is defined by a regional highly-deformed zone that extends from the southern Istmina deformed belt to the Dabeiba area, and

further to the northwest towards the Urabá Gulf. The younger AHe ages presented here document ongoing exhumation of the Western Cordillera rocks since the Late Miocene-Pliocene until present, which together with the occurrence of great-magnitude surface uplift mainly recorded in the Eastern Cordillera and southern massifs of Colombia (Garzon and Quetame), as well as the coexistence of an active magmatic arc, suggest that Nazca subduction beneath South-America initiated right after the Middle Miocene collisional episode and is still active today.

5. References

ANH-Universidad de Caldas, 2008. Estratigrafía de la Formación La Paila, un potencial reservorio de hidrocarburos en la Cuencua Cauca-Patía.

Bacon, C.D., Silvestro, D., Jaramillo, C., Smith, B.T., Chakrabarty, P., Antonelli, A., 2015. Biological evidence supports an early and complex emergence of the Isthmus of Panama. Proc. Natl. Acad. Sci. U. S. A. 112, 6110–6115.

Bayona, G., Cardona, A., Jaramillo, C., Mora, A., Montes, C., Valencia, V., Ayala, C., Montenegro, O., Ibañez-Mejia, M., 2012. Early Paleogene magmatism in the northern Andes: Insights on the effects of Oceanic Plateau–continent convergence. Earth Planet. Sci. Lett. 331–332, 97–111.

Bernet, M., Spiegel, C., 2004. Introduction: Detrital thermochronology, in: Bernet, M., Spiegel, C. (Eds.), Detrital Thermochronology - Provenance Analysis, Exhumation, and Landscape Evolution of Mountain Belts, Geological Society of America Special Paper 378. Boulder, Colorado, pp. 1–6.

Boutelier, D., Oncken, O., Cruden, A., 2012. Fore-arc deformation at the transition between collision and subduction: Insights from 3-D thermomechanical laboratory experiments. Tectonics 31, TC2015. doi:10.1029/2011TC003060

Brewer, I.D., Burbank, D.W., Hodges, K. V., 2003. Modelling detrital cooling-age populations: insights from two Himalayan catchments. Basin Res. 15, 305–320. doi:10.1046/j.1365-2117.2003.00211.x

Buchs, D.M., Arculus, R.J., Baumgartner, P.O., Baumgartner-Mora, C., Ulianov, A., 2010. Late Cretaceous arc development on the SW margin of the Caribbean Plate: Insights from the Golfito, Costa Rica, and Azuero, Panama, complexes. Geochemistry, Geophys. Geosystems 11, 1–35. doi:10.1029/2009GC002901

Buchs, D.M., Baumgartner, P.O., Baumgartner-Mora, C., Flores, K., Bandini, A.N., 2011. Upper Cretaceous to Miocene tectonostratigraphy of the Azuero area (Panama) and the discontinuous accretion and subduction erosion along the Middle American margin. Tectonophysics 512, 31–46. doi:10.1016/j.tecto.2011.09.010

Burke, K., 1988. Tectonic evolution of the Caribbean. Annu. Rev. Earth Planet. Sci. 16, 201–230. doi:10.1146/annurev.earth.16.1.201

Cardona, A., Valencia, V., Bayona, G., Duque, J., Ducea, M.N., Gehrels, G.E., Jaramillo, C., Montes, C., Ojeda, G., Ruiz, J., 2011. Early-subduction-related orogen in the northern Andes: Turonian to Eocene magmatic and provenance record in the Santa Marta Massif and Rancheria Basin, northern Colombia. Terra Nov. 23, 26–34.

Cawood, P.A., Kröner, A., Collins, W.J., Kusky, T.M., Mooney, W.D., Windley, B.F., 2009. Accretionary orogens through Earth history, in: Cawood, P.A., Kröner, A. (Eds.), Earth Accretionary Systems in Space and Time. Geological Society, London, Special Publications, 318, 1-36.

Cediel, F., Shaw, R.P., 2003. Tectonic Assembly of the Northern Andean Block. eds., Circum-Gulf Mex. Caribb. Hydrocarb. habitats, basin Form. plate tectonics 79, 815–848.

Chang, Z., Vervoort, J.D., McClelland, W.C., Knaack, C., 2006. U-Pb dating of zircon by LA-ICP-MS. Geochemistry, Geophys. Geosystems 7.

Chiarabba, C., De Gori, P., Faccenna, C., Speranza, F., Seccia, D., Dionicio, V., Prieto, G.A., 2015. Subduction system and flat slab beneath the Eastern Cordillera of Colombia. Geochemistry, Geophys. Geosystems 17, 16–27. doi:10.1002/2014GC005684.Key

Cloos, M., 1993. Lithospheric buoyancy and collisional orogenesis: Subduction of oceanic plateaus, continental margins, island arcs, spreading ridges, and seamounts. Geol. Soc. Am. Bull. 105, 715–737. doi:10.1130/0016-7606(1993)105<0715

Coates, A.G., Collins, L.S., Aubry, M.-P., Berggren, W. a., 2004. The Geology of the Darien, Panama, and the late Miocene-Pliocene collision of the Panama arc with northwestern South America. Geol. Soc. Am. Bull. 116, 1327. doi:10.1130/B25275.1

Dickin, A.P., 2005. Radiogenic Isotope Geology, 2nd Ed. ed. Cambridge University Press, New York.

Dickinson, W.R., 1985. Interpreting provenance relations from detrital modes of Sandstones, in: Zuffa, G.G. (Ed.), Provenance of Arenites. pp. 333–361.

Dodson, M.H., 1973. Closure Temperature in Cooling Geochronological and Petrological Systems. Contrib. to Mineral. Petrol. 40, 259–274.

Donelick, R.A., O'Sullivan, P.B., Ketcham, R.A., 2005. Apatite Fission-Track Analysis, in: Reiners, P.W., Ehlers, T.A. (Eds.), Low-Temperature Thermochronology, Reviews in Mineralogy and Geochemistry. pp. 49–94.

Dumitru, T.A., 1993. New computer-automated microscope stage system for fission-track

analysis. Nucl. Radiat. Meas. 21, 575–580.

Dumitru, T.A., 1991. Effects of subduction parameters on geothermal gradients in forearcs, with an application to Franciscan subduction in California. J. Geophys. Res. 96, 621–641.

Dunkl, I., 2002. Trackkey: A windows program for calculation and graphical presentation of fission track data. Comput. Geosci. 28, 3–12.

Duque-Caro, H., 1990a. The Choco Block in the northwestern corner of South America : Structural, tectonostratigraphic, and paleogeographic implications. J. South Am. Earth Sci. 3, 71–84.

Duque-Caro, H., 1990b. Neogene stratigraphy, paleoceanography and paleobiogeography in northwest South America and evolution of the Panama Seaway. Palaeogeogr. Palaeoclimatol. Palaeoecol. 77, 203–234.

Escalona, A., Mann, P., 2011. Tectonics, basin subsidence mechanisms, and paleogeography of the Caribbean-South American plate boundary zone. Mar. Pet. Geol. 28, 8–39. doi:10.1016/j.marpetgeo.2010.01.016

Farley, K.A., 2002. (U-Th)/He dating: Techniques, calibrations, and applications. Rev. Mineral. Geochemistry 47, 819–844.

Farley, K.A., 2000. Helium diffusion from apatite: General behavior as illustrated by Durango fluorapatite. J. Geophys. Res. 105, 2903–2914.

Farley, K.A., Wolf, R.A., Silver, L.T., 1996. The effects of long alpha-stopping distances on (U-Th)/He ages. Geochim. Cosmochim. Acta 60, 4223–4229.

Farris, D.W., Jaramillo, C., Bayona, G., Restrepo-Moreno, S.A., Montes, C., Cardona, A., Valencia, V., 2011. Fracturing of the Panamanian Isthmus during initial collision with South America. Geology 39, 1007–1010.

Faure, G., 1986. Principles of Isotope Geology, 2nd Ed. ed. Wiley, New York.

Fleischer, R.L., Price, P.B., Walker, R.M., 1975. Nuclear Tracks in Solids: Principles and Applications. University of California Press, Berkeley.

Flowers, R.M., Shuster, D.L., Wernicke, B.P., Farley, K.A., 2007. Radiation damage control on apatite (U-Th)/He dates from the Grand Canyon region, Colorado Plateau. Geology 35, 447–450.

Folk, R.L., 1980. Petrology of Sedimentary Rocks. Hemphill Publishing Company, Austin, Texas.

Galbraith, R.F., 1981. On statistical models for fission track counts. Math. Geol. 13, 471–478.

Gallagher, K., Brown, R., Johnson, C., 1998. Fission Track Analysis and its Applications to Geological Problems. Annu. Rev. Earth Planet. Sci. 26, 519–572.

Gansser, A., 1973. Facts and theories on the Andes. Geol. Soc. London 129, 93–131.

Garver, J.I., Brandon, M.T., Roden-Tice, M., Kamp, P.J.J., 1999. Exhumation history of orogenic highlands determined by detrital fission-track thermochronology, in: Ring, U., Brandon, M.T., Lister, G.S., Willett, S.D. (Eds.), Exhumation Processes: Normal Faulting, Ductile Flow and Erosion. Geological Society, London, Special Publications, 154. pp. 283–304.

Garzanti, E., 2016. From static to dynamic provenance analysis - sedimentary petrology upgraded. Sediment. Geol. 336, 3–13. doi:10.1016/j.sedgeo.2015.07.010

Gehrels, G.E., 2012. Detrital zircon U-Pb geochronology: current methods and new opportunities, in: Busby, C.J., Azor-Pérez, A. (Eds.), Tectonics of Sedimentary Basins: Recent Advances. Wiley-Blackwell, pp. 47–62.

Geotec, 2003. Geología de los Cinturones Sinú-San Jacinto. Planchas 50 Puerto Escondido, 51 Lorica, 59 Mulatos, 60 Canalete, 61 Montería, 69 Necoclí, 70 San Pedro de Urabá, 71 Planeta Rica, 79 Turbo, 80 Tierralta.

Gleadow, A.J.W., 1981. Fission-track dating methods: what are the real alternatives? Nucl. Tracks 5, 3–14.

Gleadow, A.J.W., Duddy, I.R., 1981. A natural long-term tracks annealing experiments for apatite. Nucl. Tracks 5, 169–174.

Gómez, E., Jordan, T.E., Allmendinger, R.W., Hegarty, K., Kelley, S., 2005. Syntectonic Cenozoic sedimentation in the northern middle Magdalena Valley Basin of Colombia and implications for exhumation of the Northern Andes. Bull. Geol. Soc. Am. 117, 547–569. doi:10.1130/B25454.1

Gómez, E., Jordan, T.E., Allmendinger, R.W., Hegarty, K., Kelley, S., Heizler, M., 2003. Controls on architecture of the Late Cretaceous to Cenozoic southern Middle Magdalena Valley Basin, Colombia. Geol. Soc. Am. Bull. 115, 131–147.

Gómez, J., Montes, N.E., Alcárcel, F.A., Ceballos, J.A., 2015. Catálogo de dataciones radiométricas de Colombia en ArcGIS y Google Earth, in: Gómez, J., Almanza, M.F. (Eds.), Compilando La Geología de Colombia: Una Visión a 2015. Servicio Geológico

Colombiano, Bogotá, pp. 51–333.

Guenthner, W.R., Reiners, P.W., Ketcham, R.A., Nasdala, L., Giester, G., 2013. Helium diffusion in natural zircon: Radiation damage, anisotropy, and the interpretation of zircon (U-Th)/He thermochronology. Am. J. Sci. 313, 145–198.

Haffer, J., 1967. On the geology of the Urabá and northern Chocó regions, northwestern Colombia.

Hasebe, N., Barbarand, J., Jarvis, K., Carter, A., Hurford, A.J., 2004. Apatite fission-track chronometry using laser ablation ICP-MS. Chem. Geol. 207, 135–145.

Henry, S.G., Pollack, H.N., 1988. Terrestrial heat flow aobve the Andean subduction zone in Bolivia and Peru. J. Geophys. Res. 93, 15,153-15,162.

Horton, B.K., Parra, M., Saylor, J.E., Nie, J., Mora, A., Stockli, D.F., Strecker, M., 2010. Resolving uplift of the northern Andes using detrital zircon age signatures. GSA Today 20, 4–10. doi:10.1130/GSATG76A.1

Howard, J.L., 1993. The statistics of counting clasts in rudites: a review, with examples from the upper Palaeogene of southern California, USA. Sedimentology 40.

Hurford, A.J., 1990. Standardization of fission-track dating calibration: recommendation by the Fission Track Working Group of the I.U.G.S. Subcommission on Geochronology. Chem. Geol. 80, 171–178.

Hurford, A.J., Green, P.F., 1983. The zeta age calibration of fission-track dating. Isot. Geosci. 1, 285–317.

Ibaraki, M., 1997. Closing of the Central American Seaway and Neogene coastal upwelling along the Pacific coast of South America. Tectonophysics 281, 99–104. doi:10.1016/S0040-1951(97)00161-3

Iturralde-Vinent, M.A., MacPhee, R.D.E., 1999. Paleogeography of the Caribbean Region: Implications for Cenozoic Biogeography. Bull. Am. Museum Nat. Hist. 238, 95.

Janoušek, V., Farrow, C.M., Erban, V., 2006. Interpretation of whole-rock geochemical data in igneous geochemistry: introducing Geochemical Data Toolkit (GCDkit). J. Petrol. 47, 1255–1259.

Kay, S.M., Coira, B.L., 2009. Shallowing and steepening subduction zones, continental lithospheric loss, magmatism, and crustal flow under the central Andean Altiplano-Puna Plateau, in: Backbone of the Americas: Shallow Subduction, Plateau Uplift and Ridge and

Terrane Collision. Geological Society of America Memoir 204. pp. 229–260. doi:10.1130/2009.1204(11).

Kerr, A.C., Marriner, G.F., Tarney, J., Nivia, A., Saunders, A.D., Thirlwall, M.F., Sinton, C.W., 1997. Cretaceous Basaltic Terranes in Western Colombia : Elemental, Chronological and Sr – Nd Isotopic Constraints on Petrogenesis. J. Petrol. 38, 677–702.

Kerr, A.C., Tarney, J., Marriner, G.F., Klaver, G.T.H., Saunders, A.D., 1996. The geochemistry and tectonic setting of late Cretaceous Caribbean and Colombian volcanism. J. South Am. Earth Sci. 9, 111–120.

Ketcham, R.A., 2005. Forward and inverse modeling of low-temperature thermocronometry data, in: Reiners, P.W., Ehlers, T.A. (Eds.), Low-Temperature Thermochronology. Reviews in mineralogy and Geochemistry, Volume 58, pp. 275–314.

Ketcham, R.A., Carter, A., Donelick, R.A., Barbarand, J., Hurford, A.J., 2007. Improved modeling of fission-track annealing in apatite. Am. Mineral. 92, 799–810. doi:10.2138/am.2007.2281

Kusky, T.M., Windley, B.F., Safonova, I., Wakita, K., Wakabayashi, J., Polat, A., Santosh, M., 2013. Recognition of ocean plate stratigraphy in accretionary orogens through Earth history : A record of 3.8 billion years of sea floor spreading, subduction, and accretion. Gondwana Res. 24, 501–547. doi:10.1016/j.gr.2013.01.004

Leal-Mejía, H., 2011. Phanerozoic gold metallogeny in the Colombian Andes: A tectono-magmatic approach. Universidad de Barcelona.

Lonsdale, P., 2005. Creation of the Cocos and Nazca plates by fission of the Farallon plate. Tectonophysics 404, 237–264.

Ludwig, K.R., 2003. User's Manual for Isoplot 3.00. A Geochronological Toolkit for Microsoft Excel. Berkeley Geochronol. Cent. Spec. Publ. 4, 70.

Mange, M.A., Maurer, H.F.W., 1992. Heavy minerals in color. Chapman & Hall, London.

Mann, P., 1995. Geologic and tectonic development of the Caribbean plate boundary in southern Central America. Geological Society of America, Special Papers, 295.

Meesters, A.G.C.A., Dunai, T.J., 2005. A noniterative solution of the (U-Th)/He age equation. Geochemistry, Geophys. Geosystems 6, Q04002. doi:10.1029/2004GC000834

Montes, C., Bayona, G., Cardona, A., Buchs, D.M., Silva, C.A., Morón, S., Hoyos, N., Ramírez, D.A., Jaramillo, C., Valencia, V., 2012a. Arc-continent collision and orocline formation:

Closing of the Central American seaway. J. Geophys. Res. Solid Earth 117, B04105. doi:10.1029/2011JB008959

Montes, C., Cardona, A., Jaramillo, C., Pardo, A., Silva, J.C., Valencia, V., Ayala, C., Pérez-Angel, L.C., Rodriguez-Parra, L.A., Ramirez, V., Niño, H., 2015. Middle Miocene closure of the Central American Seaway. Science (80-.). 348, 226–229. doi:10.1126/science.aaa2815

Montes, C., Cardona, A., McFadden, R., Moron, S.E., Silva, C.A., Restrepo-Moreno, S.A., Ramirez, D.A., Hoyos, N., Wilson, J., Farris, D.W., Bayona, G., Jaramillo, C., Valencia, V., Bryan, J., Flores, J.A., 2012b. Evidence for middle Eocene and younger land emergence in central Panama: Implications for Isthmus closure. Geol. Soc. Am. Bull. 124, 780–799. doi:10.1130/B30528.1

Mora, A., Reyes-Harker, A., Rodriguez, G., Tesón, E., Ramirez-Arias, J.C., Parra, M., Caballero, V., Mora, J.P., Quintero, I., Valencia, V., Ibañez, M., Horton, B.K., Stockli, D.F., 2013. Inversion tectonics under increasing rates of shortening and sedimentation: Cenozoic example from the Eastern Cordillera of Colombia, in: Nemčok, M., Mora, A., Cosgrove, J.W. (Eds.), Thick-Skin-Dominated Orogens: From Initial Inversion to Full Accretion. Geological Society of London, Special Publication, 377, London, pp. 411–442. doi:10.1144/SP377.6

Morton, A.C., 1985. Heavy minerals in provenance studies, in: Zuffa, G.G. (Ed.), Provenance of Arenites. Springer Netherlands, pp. 249–277.

Noriega-Londoño, S., Caballero, J.H., Rendón Rivera, A., 2013. Estudio morfotectónico de un tramo del río Herradura entre Frontino y Abriaquí, Cordillera Occidental de Colombia. Boletín Ciencias la Tierra 33, 71–84.

O' Dea, A., Lessios, H.A., Coates, A.G., Eytan, R.I., Restrepo-Moreno, S.A., Cione, A.L., Collins, L.S., de Queiroz, A., Farris, D.W., Norris, R.D., Stallard, R.F., Woodburne, M.O., Aguilera, O., Aubry, M.-P., Berggren, W.A., Budd, A.F., Cozzuol, M.A., Coppard, S.E., Duque-Caro, H., Finnegan, S., Gasparini, G.M., Grossman, E.L., Johnson, K.G., Keigwin, L.D., Knowlton, N., Leigh, E.G., Leonard-Pingel, J.S., Marko, P.B., Pyenson, N.D., Rachello-Dolmen, P.G., Soibelzon, E., Soibelzon, L., Todd, J.A., Vermeij, G.J., Jackson, J.B.C., 2016. Formation of the Isthmus of Panama. Sci. Adv. 2, e1600883. doi:10.1126/sciadv.1600883

Pardo-Casas, F., Molnar, P., 1987. Relative motion of the Nazca (Farallon) and South American Plates since late Cretaceous time. Tectonics 6, 233–248.

Pardo-Trujillo, A., Restrepo-Moreno, S.A., Vallejo, D.F., Flores, J.A., Trejos, R., Foster, D.A., Barbosa-Espitia, A.A., Bernet, M., Marín-Cerón, M.I., Kamenov, G.D., 2015. New thermotectonic and paleo-environmental constraints from the Western Cordillera and associated sedimentary basins (Northern Andes, Colombia): The birth of a major orographic barrier and the Choco bio-geopragphic region?, in: GSA Annual Meeting. Baltimore, Maryland, USA.

Parra, M., Mora, A., Jaramillo, C., Strecker, M.R., Sobel, E.R., Quiroz, L., Rueda, M., Torres, V., 2009a. Orogenic wedge advance in the northern Andes: Evidence from the Oligocene-Miocene sedimentary record of the Medina Basin, Eastern Cordillera, Colombia. Geol. Soc. Am. Bull. 121, 780–800. doi:10.1130/B26257.1

Parra, M., Mora, A., Jaramillo, C., Torres, V., Zeilinger, G., Strecker, M.R., 2010. Tectonic controls on Cenozoic foreland basin development in the north-eastern Andes, Colombia. Basin Res. 22, 874–903.

Parra, M., Mora, A., López, C., Rojas, L.E., Horton, B.K., 2012. Detecting earliest shortening and deformation advance in thrust-belt hinterlands: Example from the Colombian Andes. Geology 40, 171–174.

Parra, M., Mora, A., Sobel, E.R., Strecker, M.R., González, R., 2009b. Episodic orogenic front migration in the northern Andes: Constraints from low-temperature thermochronology in the Eastern Cordillera, Colombia. Tectonics 28, TC4004. doi:10.1029/2008TC002423

Pindell, J.L., Kennan, L., 2009. Tectonic evolution of the Gulf of Mexico, Caribbean and northern South America in the mantle reference frame : an update, in: James, K.H., Lorente, M.A., Pindell, J.L. (Eds.), The Geology and Evolution of the Region between North and South America, Geological Society of London, Special Publication. pp. 1–60.

Pubellier, M., Meresse, F., 2013. Phanerozoic growth of Asia: Geodynamic processes and evolution. J. Asian Earth Sci. 72, 118–128. doi:10.1016/j.jseaes.2012.06.013

Ramírez, D.A., Foster, D.A., Min, K., Montes, C., Cardona, A., Sadove, G., 2016. Exhumation of the Panama basement complex and basins: Implications for the closure of the Central American seaway. Geochemistry, Geophys. Geosystems 17, 1758–1777. doi:10.1002/2016GC006289

Ramos, V.A., 2010. The tectonic regime along the Andes: Present-day and Mesozoic regimes. Geol. J. 45, 2–25.

Ramos, V.A., 1999. Plate tectonic setting of the Andean Cordillera. Episodes 22, 183–190.

Reiners, P.W., 2005. Zircon (U-Th)/He Thermochronometry, in: Reiners, P.W., Ehlers, T.A. (Eds.), Low-Temperature Thermochronology, Reviews in Mineralogy and Geochemistry. pp. 151–179. doi:10.2138/rmg.2005.58.6

Reiners, P.W., Brandon, M.T., 2006. Using Thermochronology To Understand Orogenic Erosion. Annu. Rev. Earth Planet. Sci. 34, 419–466. doi:10.1146/annurev.earth.34.031405.125202

Reiners, P.W., Ehlers, T.A., 2005. Low-Temperature Thermochronology: Techniques, Interpretations, Applications. Reviews in mineralogy and Geochemistry, Volume 58. doi:10.2138/rmg.2005.58.6

Reiners, P.W., Ehlers, T.A., Zeitler, P.K., 2005. Past, Present and Future of Thermochronology, in: Reiners, P.W., Ehlers, T.A. (Eds.), Low-Temperature Thermochronology, Reviews in Mineralogy and Geochemistry. pp. 1–18. doi:10.2138/rmg.2005.58.6

Restrepo-Moreno, S.A., Foster, D.A., Stockli, D.F., Parra-Sánchez, L.N., 2009. Long-term erosion and exhumation of the "Altiplano Antioqueño", Northern Andes (Colombia) from apatite (U–Th)/He thermochronology. Earth Planet. Sci. Lett. 278, 1–12. doi:10.1016/j.epsl.2008.09.037

Restrepo-Moreno, S.A., Vinasco, C., Foster, D.A., Min, K., Noriega, S., Bernet, M., Marín-Cerón, M.I., Bermúdez, M., Botero, M., 2015. Cenozoic accretion and morpho-tectonic response in the northern Andes (Colombia) through low-temperature thermochronology analyses/modeling, in: GSA Annual Meeting. Baltimore, Maryland, USA.

Restrepo, J.J., Toussaint, J.F., 1988. Terranes and Continental Accretion in the Colombian Andes. Episodes 11, 189–193.

Reyes-Harker, A., Ruiz-Valdivieso, C.F., Mora, A., Ramirez-Arias, J.C., Rodriguez, G., de la Parra, F., Caballero, V., Parra, M., Moreno, N., Horton, B.K., Saylor, J.E., Silva, A., Valencia, V., Stockli, D., Blanco, V., 2015. Cenozoic paleogeography of the Andean foreland and retroarc hinterland of Colombia. Am. Assoc. Pet. Geol. Bull. 99, 1407–1453. doi:10.1306/06181411110

Rodríguez-García, G., Bermúdez-Cordero, J.G., 2015. Petrography, geochemistry and age of

Cerro Frontino Gabro. Bol. Ciencias la Tierra 38, 25–40.

Rodríguez, G., Arango, M.I., 2013. Formación Barroso: Arco Volcánico Toleítico y Diabasas de San José de Urama: Un Prisma Acrecionario T-MORB en el Segmento Norte de la Cordillera Occidental de Colombia. Boletín Ciencias la Tierra 33, 17–38.

Rodríguez, G., Arango, M.I., Bemúdez, J.G., 2012. Batolito de Sabanalarga, Plutonismo de Arco en la Zona de Sutura entre las Cortezas Oceánica y Continental de los Andes del Norte. Boletín Ciencias la Tierra 32, 81–98.

Rodríguez, G., Arango, M.I., Zapata, G., Bermúdez-Cordero, J.G., 2016. Estratigrafía, Petrografía y Análisis Multi-Método de Procedencia de la Formación Guineales, Norte de la Cordillera Occidental de Colombia. Boletín Geol. 38, 101–124.

Rodríguez, G., Zapata, G., 2012. Características del plutonismo Mioceno Superior en el segmento norte de la Cordillera Occidental e implicaciones tectónicas en el modelo geológico del noroccidente Colombiano. Bol. Ciencias la Tierra 31, 5–22.

Rodríguez, G., Zapata, G., Gómez, J.F., 2013. Geología de la plancha 114 - Dabeiba. Escala 1:100.000.

Ruhl, K.W., Hodges, K. V., 2005. The use of detrital mineral cooling ages to evaluate steady state assumptions in active orogens: An example from the central Nepalese Himalaya. Tectonics 24, TC4015. doi:10.1029/2004TC001712

Schütte, P., Chiaradia, M., Beate, B., 2010. Geodynamic controls on Tertiary arc magmatism in Ecuador: Constraints from U-Pb zircon geochronology of Oligocene-Miocene intrusions and regional age distribution trends. Tectonophysics 489, 159–176.

Sinton, C.W., Duncan, R.A., Storey, M., Lewis, J., Estrada, J.J., 1998. An oceanic flood basalts province within the Caribbean plate. Earth Planet. Sci. Lett. 155, 221–235.

Sláma, J., Košler, J., Condon, D.J., Crowley, J.L., Gerdes, A., Hanchar, J.M., Hortswood, M.S.A., Morris, G.A., Nasdala, L., Norberg, N., Schaltegger, U., Schoene, B., Tubrett, M.N., Whitehouse, M.J., 2008. Plešovice zircon—a new natural reference material for U–Pb and Hf isotopic microanalysis. Chem. Geol. 249, 1–35.

Sobel, E.R., Seward, D., 2010. Influence of etching conditions on apatite fission-track etch pit diameter. Chem. Geol. 271, 59–69. doi:10.1016/j.chemgeo.2009.12.012

Somoza, R., 1998. Updated Nazca (Farallon) - South America relative motions during the last 40 My: implications for mountain building in the central Andean region. J. South Am.

Earth Sci. 11, 211–215.

Somoza, R., Ghidella, M.E., 2012. Late Cretaceous to recent plate motions in western South America revisited. Earth Planet. Sci. Lett. 331–332, 152–163. doi:10.1016/j.epsl.2012.03.003

Spikings, R.A., Cochrane, R., Villagómez, D., Van der Lelij, R., Vallejo, C., Winkler, W., Beate, B., 2015. The geological history of northwestern South America: From Pangaea to the early collision of the Caribbean Large Igneous Province (290 – 75Ma). Gondwana Res. 27, 95–139. doi:10.1016/j.gr.2014.06.004

Spikings, R.A., Simpson, G., 2014. Rock uplift and exhumation of continental margins by the collision, accretion, and subduction of buoyant and topographically prominent oceanic crust. Tectonics 33, 1–21. doi:10.1002/2013TC003425.Received

Suter, F., Sartori, M., Neuwerth, R., Gorin, G., 2008. Structural imprints at the front of the Chocó-Panamá intender: Field data from the North Cauca Valley Basin, Central Colombia. Tectonophysics 460, 134–157.

Syracuse, E.M., Maceira, M., Prieto, G.A., Zhang, H., Ammon, C.J., 2016. Multiple plates subducting beneath Colombia, as illuminated by seismicity and velocity from the joint inversion of seismic and gravity data. Earth Planet. Sci. Lett. 444, 139–149.

Tagami, T., O'Sullivan, P.B., 2005. Fundamentals of Fission-Track Thermochronology, in: Reiners, P.W., Ehlers, T.A. (Eds.), Low-Temperature Thermochronology, Reviews in Mineralogy and Geochemistry. pp. 19–47. doi:10.2138/rmg.2005.58.2

Toussaint, J.F., Restrepo, J.J., 1994. The Colombian Andes During Cretaceous Times, in: Salfity, J.A. (Ed.), Cretaceous Tectonics of the Andes. pp. 61–100.

Tsuchi, R., 1997. Marine climatic responses to Neogene tectonics of the Pacific Ocean seaways. Tectonophysics 281, 113–124.

Valencia-Giraldo, Y.P., Escobar-Arenas, L.C., Mendoza-Ramírez, J., Delgado-Sierra, D., Cárdenas-Rozo, A.L., 2016. Revisión de las localidades fosilíferas del departamento de Antioquia, Colombia. Bol. Ciencias la Tierra 40, 46–54.

Vannucchi, P., Fisher, D.M., Bier, S., Gardner, T.W., 2006. From seamount accretion to tectonic erosion; formation of Osa melange and the effects of Cocos Ridge subduction in southern Costa Rica. Tectonics 25, TC2004.

Veloza, G., Taylor, M., Mora, A., Gosse, J., 2015. Active mountain building along the eastern

Colombian Subandes: A folding history from deformed terraces across the Tame anticline, Llanos Basin. Geol. Soc. Am. Bull. 127, 1155–1173.

Vermeesch, P., 2012. On the visualization of detrital age distributions. Chem. Geol. 312–313, 190–194.

Vermeesch, P., 2009. RadialPlotter: A Java application for fission track, luminescence and other radial plots. Radiat. Meas. 44, 409–410. doi:10.1016/j.radmeas.2009.05.003

Villagómez, D., Spikings, R.A., 2013. Thermochronology and tectonics of the Central and Western Cordilleras of Colombia: Early Cretaceous–Tertiary evolution of the Northern Andes. Lithos 160–161, 228–249. doi:10.1016/j.lithos.2012.12.008

Villagómez, D., Spikings, R.A., Magna, T., Kammer, A., Winkler, W., Beltrán, A., 2011. Geochronology, geochemistry and tectonic evolution of the Western and Central cordilleras of Colombia. Lithos 125, 875–896. doi:10.1016/j.lithos.2011.05.003

von Huene, R., Scholl, D.W., 1991. Observations at convergent margins concerning sediment subduction, subduction erosion, and the growth of continental-crust. Rev. Geophys. 29, 279–316.

Webb, S.D., 2006. The Great American Biotic Interchange : Patterns and Processes. Ann. Missouri Bot. Gard. 93, 245–257.

Wegner, W., Wörner, G., Harmon, R.S., Jicha, B.R., 2011. Magmatic history and evolution of the Central American Land Bridge in Panama since Cretaceous times. Geol. Soc. Am. Bull. 123, 703–724. doi:10.1130/B30109.1

Whattam, S.A., Montes, C., Mcfadden, R.R., Cardona, A., Ramirez, D., Valencia, V., 2012. Age and origin of earliest adakitic-like magmatism in Panama: Implications for the tectonic evolution of the Panamanian magmatic arc system. Lithos 142–143, 226–244. doi:10.1016/j.lithos.2012.02.017

Wörner, G., Harmon, R.S., Wegner, W., 2009. Geochemical evolution of igneous rocks and changing magma sources during the formation and closure of the Central American land bridge of Panama, in: Kay, S.M., Ramos, V.A., Dickinson, W.R. (Eds.), Backbone of the Americas: Shallow Subduction, Plateau Uplift and Ridge and Terrane Collision. Geological Society of America Memoir 204. pp. 183–196. doi:10.1130/2009.1204(08).

Zapata, G., Rodríguez, G., 2011. Basalto de El Botón, Arco Volcánico Mioceno de Afinidad Shoshonítica al Norte de la Cordillera Occidental de Colombia. Boletín Ciencias la Tierra

30, 77–92.

Appendix 1. Principles of the Apatite Fission-Track External Detector Method

Spontaneous decay of radioactive nuclides, either alpha decay or fission decay, constitutes the basis of the entire series of methods for radiometric dating of rocks (i.e. ^{238}U – ^{206}Pb, ^{235}U – ^{207}Pb, ^{87}Rb – ^{87}Sr, ^{176}Lu – ^{176}Hf, fission-tracks, etc.). Basically, the proportional abundance of the radiogenic product (daughter nuclei) and the radioactive isotope (parent nuclei), knowing the decay rate or constant, enable to determine the approximate time since the radiometric system has been at temperatures low enough for retention of the daughter product in the mineral´s crystal lattice. (Dickin, 2005; Dodson, 1973; Faure, 1986). Among the great variety of radioisotopic systems, those with the lowest ranges of closure temperatures (< 300°C) are known as Low-Temperature Thermochronometers (Reiners and Ehlers, 2005) and are used to reconstruct thermal histories of rocks through middle-upper crustal levels (<10-15 Km), where geological processes like evolution of sedimentary basins, hydrocarbon generation, and long-term landscape evolution, can be addressed (Donelick et al., 2005; Farley, 2002; Gallagher et al., 1998; Reiners & Brandon, 2006).

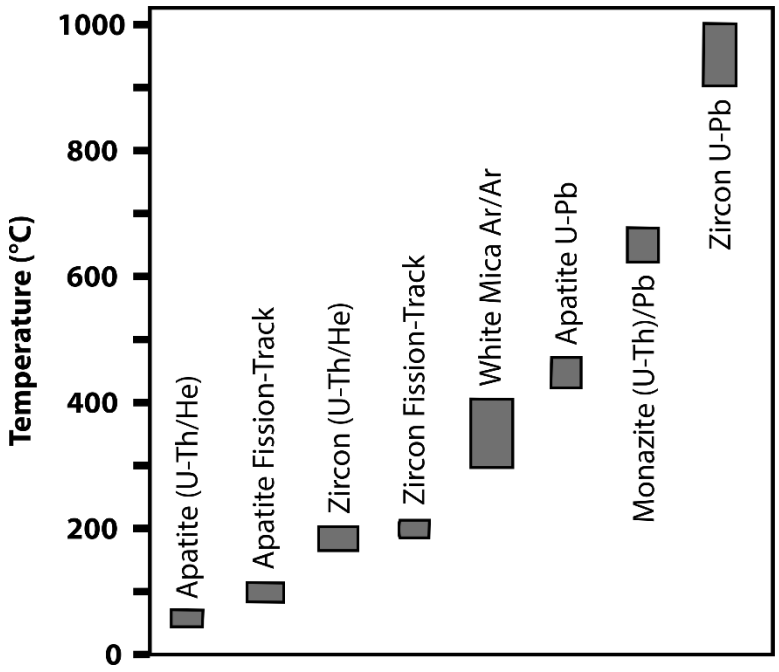

Figure 3. Estimated closure temperatures for different thermochronometers and geochronometers. Modified from (Reiners et al., 2005)

3.5.1. Apatite Fission-Track

3.5.1.1. Spontaneous Fission of ^{238}U

The radioactive isotope ^{238}U spontaneously decays by a series of α (^{4}He nuclei) and $^{-}\beta$ (transformation of a neutron into a proton and an electron, the latter being expelled from the atom) particle emissions. Additionally, nuclear fission of ^{238}U, when an unstable nucleus splits into a pair of highly charged fragments, produces a micrometric scale damage trail into the lattice of the host mineral (i.e. apatite, zircon, monazite, titanite) called latent spontaneous fission-track (Tagami and O'Sullivan, 2005). The most accepted theory about how fission-tracks are formed is the "ion explosion spike" model proposed by Fleischer et al. (1975). The model suggests that rapid moving of a positively-charged particle and consequent repulsion of the positively-ionized lattice atoms yields vacancies.

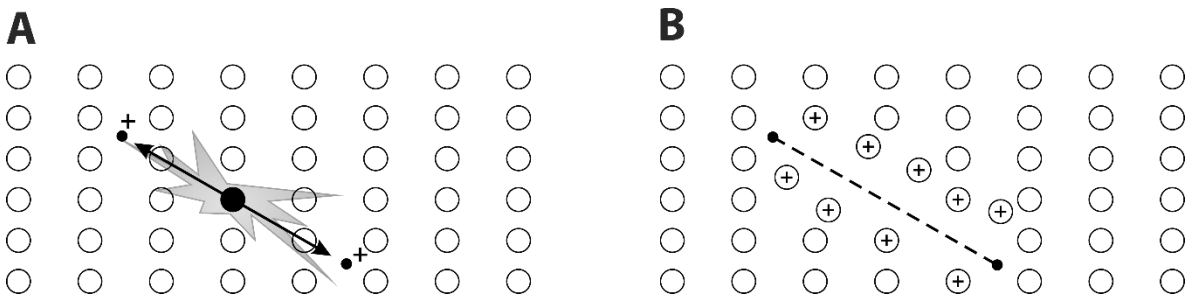

Figure 4. Schematic representation of the "ion explosion spike" model. Modified from (Gallagher et al., 1998)

3.5.1.2. Annealing of Fission-Tracks

Fission-tracks begin to anneal as they are formed at temperatures above ~100°C (Donelick et al., 2005; Reiners and Brandon, 2006). Nonetheless, both natural and laboratory experiments have demonstrated that temperatures at which fission-tracks in apatite are partially or totally annealed are also a function of the cooling rate and the chemical composition (i.e. proportional abundance of Cl, F or OH) (Ketcham et al., 2007). The intersection of tracks with a polished and etched internal surface of an apatite crystal has the form of a rhomboid called *etch-pit*. The

length of its longer axis, known as the *Dpar*, is a parameter that has empirically been suggested to constitute a proxy for the annealing kinetics of the fission-tracks (Donelick et al., 2005; Ketcham, 2005; Ketcham et al., 2007; Tagami and O'Sullivan, 2005). Therefore, the length distribution of apatite fission-tracks records a protracted cooling history of a rock sample instead of a simple cooling age through a certain closure temperature (Gallagher et al., 1998). Despite of the complexity of the kinetics for fission-track annealing, a temperature range of approximately between 60°C and 130°C, called the *Partial Annealing Zone (PAZ)*, is widely accepted in the scientific community (Gleadow and Duddy, 1981; Reiners and Brandon, 2006).

3.5.1.3. On the Visualization of Fission-Tracks

The nanometic scale of the width of natural latent fission-tracks render their observation only possible using transmission electron microscopes (TEM's). For this reason, chemical etching of fission-track host materials has been a widely used technique in order to enlarge and make them visible under an optical microscope. Fission-tracks lengths are enlarged because the atomic disordered nature of the region where they form make it more susceptible to dissolution and chemical etching than the surrounding area (Tagami and O'Sullivan, 2005). Etching with 5.5 M HNO_3 for 20 s at 21°C of apatite grains mounted and polished in an epoxy resin is the most common routine used for fission-track analysis in this mineral (Donelick et al., 2005) and was the routine adopted in the present work.

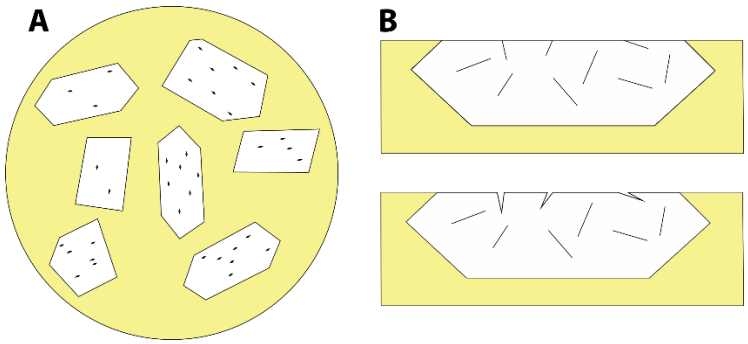

Figure 5. A) Schematic illustration of an apatite grain mount; B) Polished surface before and after etching.

3.5.1.4. Fission-Track Ages Determination

As mentioned before, apatite fission-track (AFT) dating is analogue to most commonly used geochronological systems in that, knowing the decay constant, the concentration of a parental (radioactive) and a daughter (radiogenic) isotope must be measured in a host material in order to retrieve an age. Particularly, in the AFT system, the parental isotope is ^{238}U, and the radiogenic product is not an isotope but the physical damage called fission-track. On this basis, the fundamental equation of geochronological systems,

$$D = N\left(e^{\lambda t} - 1\right) \qquad (1)$$

where *D* is the daughter or radiogenic nuclei, *N* is the abundance of the parental nuclei at the time *t*, and λ is the decay constant, has been modified for fission-track single-grain age determination in accordance with the equivalent terms.

$$N_s = \frac{\lambda_f}{\lambda_d}\,^{238}N\left(e^{\lambda_d t} - 1\right) \qquad (2)$$

Here, N_s is the number of spontaneous fission-tracks (number of tracks per unit volume), λ_f is the decay constant for spontaneous fission of ^{238}U, λ_d is the decay constant of ^{238}U by α-emission ($1.55125 \times 10^{-10} y^{-1}$), and N_{238} is the number of atoms of ^{238}U per unit volume. N_s is directly determined by counting the number of fission-tracks from a selected area within an etched apatite crystal. However, the determination of ^{238}N, the parental nuclei abundance at the time *t*, is not straightforward. For this, two principal analytical techniques are commonly used: Laser Ablation Inductively Coupled Plasma Mass Spectrometry (LA-ICP-MS) and the External Detector Method (EDM) (Donelick et al., 2005; Gallagher et al., 1998; Hasebe et al., 2004; Tagami and O'Sullivan, 2005). Here I briefly describe the EDM method, the one used in this work, following the procedures described in Donelick et al., (2005). The age calculation equations and its derivations are taken and modified from Tagami & O'Sullivan (2005).

3.5.1.5. Determination of ^{238}N using the External Detector Method (EDM) and Age Calculation

In order to measure the concentration of ^{238}U atoms, a fission-track-free external detector with low-uranium concentration (typically a muscovite sheet) is attached to an apatite grain mount and then irradiated with thermal neutrons in a nuclear reactor facility aiming to induce fission of ^{235}U.

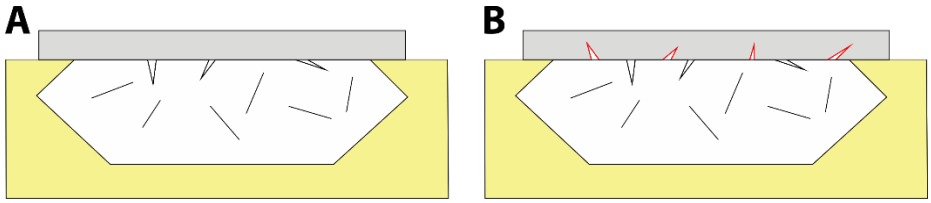

Figure 6. A) Schematic illustration showing the external detector attaching; B) Generation of induced fission-tracks after thermal neutron irradiation

Then, the resultant number of induced fission-tracks is given by:

$$N_i = {}^{235}N\sigma_f\varphi \qquad (3)$$

where ^{235}N is the abundance of ^{235}U per unit volume, σ_f is the cross-section for induced nuclear fission, and φ is the thermal neutron fluence. Therefore, after equations (2) and (3):

$$t = \frac{1}{\lambda_d}\ln\left\{1 + \left(\frac{\lambda_d}{\lambda_f}\right)\left(\frac{N_s}{N_i}\right)I\sigma_f\varphi\right\} \qquad (4)$$

where I is the isotopic ratio $^{235}U/^{238}U$ (7.2527×10^{-3}). Given that only tracks that intersect the surface of etched mounts are visible under microscope, an integrated factor of registration efficiency Q, and an integrated geometry factor of etched surface G, are added to the equation (4), thus:

$$t = \frac{1}{\lambda_d} \ln\left\{1 + \left(\frac{\lambda_d}{\lambda_f}\right)\left(\frac{\rho_s}{\rho_i}\right) I\sigma_f \varphi Q G\right\} \qquad (5)$$

where ρ_s and ρ_i are the surface density of spontaneous and induced fission-tracks respectively. Apatite fission-tracks are observed in a polished and etched surface that intersect tracks both from above and below (removed and remaining parts of the grain respectively). This registration geometry for fission-tracks is referred as a 4π geometry, where G=0.5 (Donelick et al., 2005). ρ_i is determined by counting an area on the mica detector that was directly coupled with the counted area in the apatite grain. Induced tracks hosted in the external detector are previously revealed by etching with 49% HF during 15 min at 20+-1°C (Sobel and Seward, 2010).

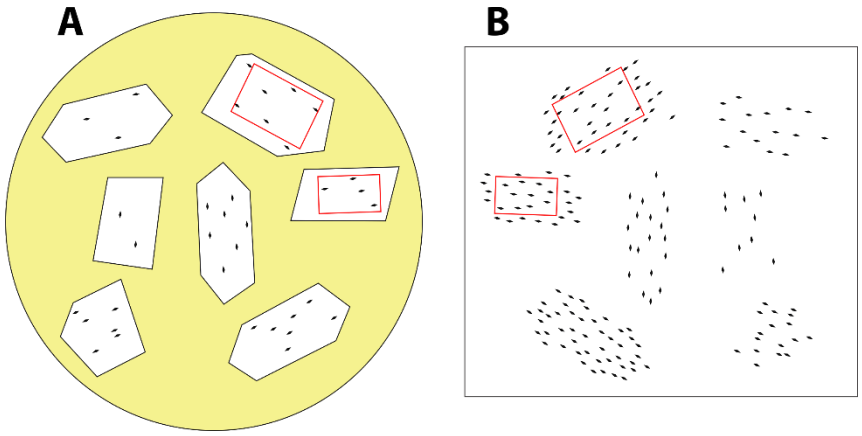

Figure 7. Schematic illustration of counting area selection. A) Apatite grains-mount; B) Mica detector

Since the measurements of the thermal-neutron-flux is extremely difficult, standard glasses with known uranium concentration, and their respective external detectors, are positioned at the top and the bottom of a series of stacked mounts being irradiated. Induced fission-track density is determined for each glass, and then a corresponding induced track density ρ_d is calculated for each sample according to its position in the sample stack by linear interpolation. Now, given that:

$$\varphi = B\rho_d \qquad (6)$$

where B is a calibration constant empirically determined, the age calculation equation results in:

$$t = \frac{1}{\lambda_d} \ln \left\{ 1 + \left(\frac{\lambda_d}{\lambda_f} \right) \left(\frac{\rho_s}{\rho_i} \right) I \sigma_f B \rho_d Q G \right\} \qquad (7)$$

Nevertheless, although it is possible to determine the parameters B, λ_f, and Q, the subcommission on Geochronology of the International Union of Geological Science (IUGS), recommend the use of the zeta ζ age calibration factor, which is based on the analysis of known ages standards (Hurford, 1990). The zeta factor is defined by:

$$\zeta = B \frac{I \sigma_f}{\lambda_f} \qquad (8)$$

Because Q is always the same between age standards and age-unknown samples, as long as they are analyzed following the same experimental conditions, this parameter is ignorable. Finally, the age calculation equation for apatite fission-track, using the EDM and the zeta age calibration method is given by:

$$t = \frac{1}{\lambda_d} \ln \left\{ 1 + \lambda_d \zeta \rho_d \left(\frac{\rho_s}{\rho_i} \right) G \right\} \qquad (9)$$

Then, the symmetrical error for an apatite single-grain age is given by:

$$\sigma_t = \sqrt{\left\{ \frac{1}{N_s} + \frac{1}{N_i} + \frac{1}{N_d} + \left(\frac{\sigma_\zeta}{\zeta} \right)^2 \right\}} \qquad (10)$$

where, N_d is the number of induced fission-tracks counted in the mica detector of the standard glasses irradiated with the samples, used to determine ρ_d. When determining the fission-track age of a bedrock sample, around 20-30 individual ages are obtained, then a pooled age is calculated using:

$$t_{pooled} = \frac{1}{\lambda_d} \ln \left\{ 1 + \lambda_d \zeta \rho_d \left(\frac{\sum N_s}{\sum N_i} \right) G \right\} \qquad (11)$$

Otherwise, when treating detrital samples, 50-100 individual ages are needed to characterize the cooling signal derived from the sources (Bernet and Spiegel, 2004; Brewer et al., 2003). In this case, a classical Probability Density Function (PDF) is used to examine data distribution (Garver et al., 1999; Ruhl and Hodges, 2005)

$$PDF = \frac{1}{\sigma_t\sqrt{2\pi}} e^{\left\{-\frac{1}{2}\left(\frac{t-t_c}{\sigma_t}\right)^2\right\}} \qquad (12)$$

where, t_c is the measured age and σ_t the respective error.